

Spectroscopic and photochemical analysis of proteorhodopsin variants from the surface of the Arctic Ocean

Jae Yong Jung^{a,1}, Ah Reum Choi^{a,1}, Yoo Kyung Lee^b, Hong Kum Lee^b, Kwang-Hwan Jung^{a,*}

^a Department of Life Science and Interdisciplinary Program of Integrated Biotechnology, Sogang University, Shinsu-Dong 1, Mapo-Gu, Seoul 121-742, Republic of Korea

^b Polar BioCenter, Korea Polar Research Institute, KORDI, Songdo Techno Park, Songdo-dong 7-50, Yeonsu-gu, Incheon 406-840, Republic of Korea

Received 18 January 2008; revised 14 April 2008; accepted 15 April 2008

Available online 22 April 2008

Edited by Peter Brzezinski

Abstract Proteorhodopsin (PR), a retinal-containing seven transmembrane helix protein, functions as a light-driven proton pump. Using PCR, we isolated 18 PR variants originating from the surface of the Arctic Ocean. Their absorption maxima were between 517 and 546 nm at pH 7. One of the isolates turned out to be identical to GPR (green light-absorbing proteorhodopsin) from Monterey Bay. Interestingly, 10 isolates had replaced a tyrosine in the retinal-binding site (Tyr200 in GPR) with Asn. They showed a slower photocycle, more blue-shifted absorption maxima at pH 10, and relatively larger ΔH and ΔS of activation of the transition between the O intermediate and the ground state compared to GPR.

© 2008 Federation of European Biochemical Societies. Published by Elsevier B.V. All rights reserved.

Keywords: Proteorhodopsin; Retinal binding site; Photocycling rate; Y200N variants; Biofilm

1. Introduction

Proteorhodopsin (PR), a type I microbial rhodopsin which functions as a light-driven proton pump using retinal photoisomerization and subsequent protein conformational changes, was first discovered in uncultivated marine γ -proteobacteria of SAR86 group [1–3]. PR families were found in Monterey Bay (Eastern Pacific Ocean), the Hawaii Ocean Time (HOT, Central North Pacific Ocean), the Antarctic Peninsula, the Mediterranean Sea, the Red Sea, and the Sargasso Sea [3–8]. Since there are only a few numbers of cultured eubacterial species bearing with PRs such as SAR11 α -proteobacteria, SAR92 γ -proteobacteria, and flavobacteria [10–12], most of the PRs have been discovered by polymerase chain reaction (PCR)-based gene survey using degenerated primers, or through genome sequencing of bacterial artificial chromosomes (BAC), fosmids, and with environmental shotgun libraries [3–8].

*Corresponding author. Fax: +82 2 704 3601.
E-mail address: kjung@sogang.ac.kr (K.-H. Jung).

¹These authors contributed equally to this work.

Abbreviations: PR, proteorhodopsin; GPR, green light-absorbing proteorhodopsin; BPR, blue light-absorbing proteorhodopsin; MBP, Monterey Bay proteorhodopsin; PCR, polymerase chain reaction; DM, *n*-dodecyl- β -D maltopyranoside

The absorption maxima of PR variants depend on the places and depth of the ocean where their hosts reside [3,5]. PR variants from the surface or from the deep ocean of the same place (e.g., Hawaiian Pacific Ocean) have different absorption maxima being spectrally tuned to usable light in their environment [3]. PR from Monterey Bay and HOT_0m have green absorption maxima (525 nm), whereas PRs from the Antarctic Ocean and HOT_75m4 have blue absorption maxima (490 nm) [3]. A single amino acid residue at the position 105 (Leu in green light-absorbing proteorhodopsin (GPR) and Gln in blue light-absorbing proteorhodopsin (BPR)), whose function was examined by structural modeling and site-directed mutagenesis, plays a key role in changing the absorption maximum in PR [5].

There are three major differences between GPR (MBP) and BPR (HOT_75m4) including the absorption maxima, photochemical reactions and proton pumping activities [9]. First, GPR absorbs green light (525 nm, pH 7), while BPR absorbs blue light (490 nm). Second, GPR shows a fast photocycle rate ($t_{1/2} < 50$ ms), while BPR shows a slower photocycle rate ($t_{1/2} > 300$ ms) than GPR [8]. Third, GPR exhibits higher light-induced proton pumping activity than BPR [9].

In this work, 18 natural PR variants from the surface of Arctic Ocean were isolated and characterized by several biophysical methods such as absorption spectroscopy, flash-induced photolysis, and light-driven proton pumping assays.

2. Materials and methods

2.1. Collection of biofilms and extraction of DNA from the marine bacteria

Biofilms were collected from the surface down to 30 cm in depth from the region around the Korean Arctic Research Station Dasan located at Ny-Alesund, Svalbard, Norway (79°N, 12°E). Total genomic DNA was extracted using an AccuPrep DNA extraction kit (Bioneer, Korea) using a modified method was used for higher plants [13,14].

2.2. PCR amplification from the bacterial genomic DNA from the Arctic Ocean

Bacterial genomic DNA was used as a template for PCR to discover new PR genes. Primers were designed using conserved N-terminal and C-terminal regions of MBP. Both non-degenerate primer (forward primer, 5'-ATGAAATTACTGATATTAGG-3'; reverse primer, 5'-AGCATTAGAAGATTCTTTAACAGC-3') and degenerate primer (forward primer, 5'-ATGAAANNATTANTGATNTT-3') were used [1,6]. PCR was performed for 40 cycles at 95 °C for 1 min, 50 °C for 1 min, and 72 °C for 2.5 min. Many PR genes were amplified with *Taq* polymerase (Vivagen, Korea), cloned into pGEM T-vector (Promega, USA), and confirmed by DNA sequencing.

2.3. Expression and purification of proteorhodopsins

To express proteorhodopsin, we used a combination of two plasmids transformed into UT5600 *Escherichia coli* strain. The pKJ900 plasmid contains a proteorhodopsin gene and a mouse *dioxygenase* gene, which can convert β -carotene into all-*trans* retinal, while the pORANGE plasmid contains β -carotene biosynthesis genes [6,15,16]. The transformed cells were induced with 1 mM IPTG (Applichem, USA) and 0.2% (+)-L-arabinose (Sigma, USA) for 24 h at 30 °C. The collected cells were sonicated (Branson sonifier 250) and the membrane fraction was treated with 1% *n*-dodecyl- β -D-maltopyranoside (DM) (Anatrace, USA). The solubilized fraction was incubated with Ni²⁺-NTA agarose (Qiagen, USA) and eluted with 0.02% DM and 250 mM imidazole (Sigma).

2.4. Absorption spectroscopy and pK_a measurements

Absorption spectroscopy was used to measure absorption maxima and to calculate pK_a values of the Schiff base counterion in purified PR. The absorption spectra were recorded with Shimadzu UV-VIS spectrophotometer (UV-2550) at pH 4, 7, and 10. In order to calculate the pK_as of the primary proton acceptor, the spectrum at pH 4.0 was used as a reference and pH was raised from 4.0 to 10. The corrected ratio of protonated and deprotonated forms at different pH values was determined as previously described [9] from the intensities of the absorption band that appears at λ_{\max} of each new component as the pH is elevated. The data were fitted to functions containing titration components ($y = A/(1 + 10^{\text{pH}-\text{pK}_a})$) using Origin Pro 6.1 [9], where *A* represents the maximal amplitude of relative absorbance changes and it indicated the fraction of the red shifted form.

2.5. Proton pumping measurements

Spheroplast vesicles were isolated by centrifugation at 30000 × g for 1 h at 4 °C (Beckman XL-90 ultracentrifuge) and washed with 10 ml of 10 mM NaCl, 10 mM MgSO₄ · 7H₂O, 100 mM CaCl₂ [9]. Samples were illuminated at 100 W/m² intensity through the short wave cutoff filter (>440 nm, Sigma Koki SCF-50S-44Y, Japan) in combination with focusing convex lens and heat-protecting (CuSO₄) filter and the pH values were monitored by Horiba pH meter F-51.

2.6. Laser-induced absorption difference spectroscopy

Flash-induced absorbance changes were measured on RSM 1000 (Olis, USA) spectrometer. The actinic flash was from an Nd-YAG pulse laser (Continuum, MinilightII, 532 nm, 6 ns, 25 mJ). Nine to 36 signals were averaged for measuring the rate of formation and decay of the photointermediates. Purified membranes were incorporated into 7% polyacrylamide gels, which were soaked in 50 mM Tris, 150 mM NaCl at pH 9.0 [17].

3. Results

3.1. Proteorhodopsin variants from the Arctic Ocean share many residues with MBP

In total, 18 PR variants were isolated from the genomic DNA of the Arctic Ocean. Fourteen PR variants found by non-degenerate primers were named NPR and four variants found by degenerate primers were named DPR (Table 1). PR genes from the Arctic Ocean can be divided into two groups: the first group has high homology with MBP (Fig. 1). While the second group (DPR2 and 4, sequences not shown) is more similar to Mediterranean PRs. NPR1 exhibited exactly the same amino acid sequences as MBP which was the first reported proteorhodopsin reported in the literature [2]. The amino acid sequence alignment shows that 16 PRs of the 1st group differ from each other at 23 positions out of 249 positions (Fig. 1). Among these, 11 positions were located in the helices E and F, and three positions are in the retinal binding pocket. Interestingly, Tyr200 of the retinal binding site in the helix F is replaced with Asn in 10 out of the 16 PRs of the first group.

3.2. All PR isolates from the Arctic region absorb mainly green light

The surface water around the Korean Arctic Research Station where the cells were collected has the pH of 7.8 and the temperature of 4.5 °C [18]. The absorption maxima of all the PR isolates were between 517 and 546 nm at pH 7 (Table 1), which falls into the green light region. NPR1 absorbs light maximally at 549 and 517 nm, at pH 4 and 10, respectively (Fig. 2). The most blue-shifted PR variant, NPR7, displayed $\lambda_{\max} = 517$ at pH 4 and 498 nm at pH 10 (Fig. 2) while for NPR14, the most red-shifted PR variant, the corresponding λ_{\max} values were 555 and 529 nm, respectively (Fig. 2). The emitted colors of these three PR isolates at neutral pH are illustrated in Fig. 2. NPR7 seems to be unstable at high pH, probably due to the additional mutation N220D in the helix G. Overall, NPR14 has five residues different from those in NPR1. At pH 10, nine PRs are more blue-shifted compared to GPR and seven PRs are red-shifted (Table 1). Interestingly,

Table 1
The absorption maxima, the pK_as of the Schiff base counterion, the photocycle rates and the proton pumping activities of PRs

Name	λ_{\max} (pH 4)	λ_{\max} (pH 7)	λ_{\max} (pH 10)	pK _a	M decay (ms)	O decay (ms)	Pumping rate (10 ⁻³) ^a	Mutation
NPR1	549	525	517	7.5	8	46	10.0	No
NPR2	551	540	521	7.5	ND	82	4.5	No
NPR3	533	529	505	7.1	30	860	<0.1	Yes
NPR4	528	523	513	7.7	44	2240	<0.1	Yes
NPR5	533	528	519	7.1	44	7521	<0.1	Yes
NPR6	528	523	502	7.2	35	489	<0.1	Yes
NPR7	517	514	498	8.1	53	159	<0.1	Yes
NPR8	530	528	507	7.6	36	1342	<0.1	Yes
NPR9	525	522	507	8.2	56	513	<0.1	Yes
NPR10	523	517	513	7.5	213	564	<0.1	Yes
NPR11	539	521	517	6.5	1.4	61	<0.1	No
NPR12	551	546	524	7.8	2.6	112	1.9	No
NPR13	548	532	522	6.8	10	53	1.0	No
NPR14	555	538	529	7.7	9	140	0.7	No
DPR1	542	537	509	7.7	45	1698	<0.1	Yes
DPR2	546	523	519	7.4	21	108	1.6	No
DPR3	524	524	506	7.9	ND	497	<0.1	Yes
DPR4	547	532	520	7.8	15	186	<0.1	No
BPR	531	499	489	7.4	ND	136	1.0	No

The M decays were fitted using single exponential functions. The O decays were fitted to bi-exponential functions and only the major components of the fit are shown. The last column indicates the presence of the Y200N replacement.

^aProton pumping rate = $\Delta[H^+]$ (mol)/amount of PR (mol)/s.

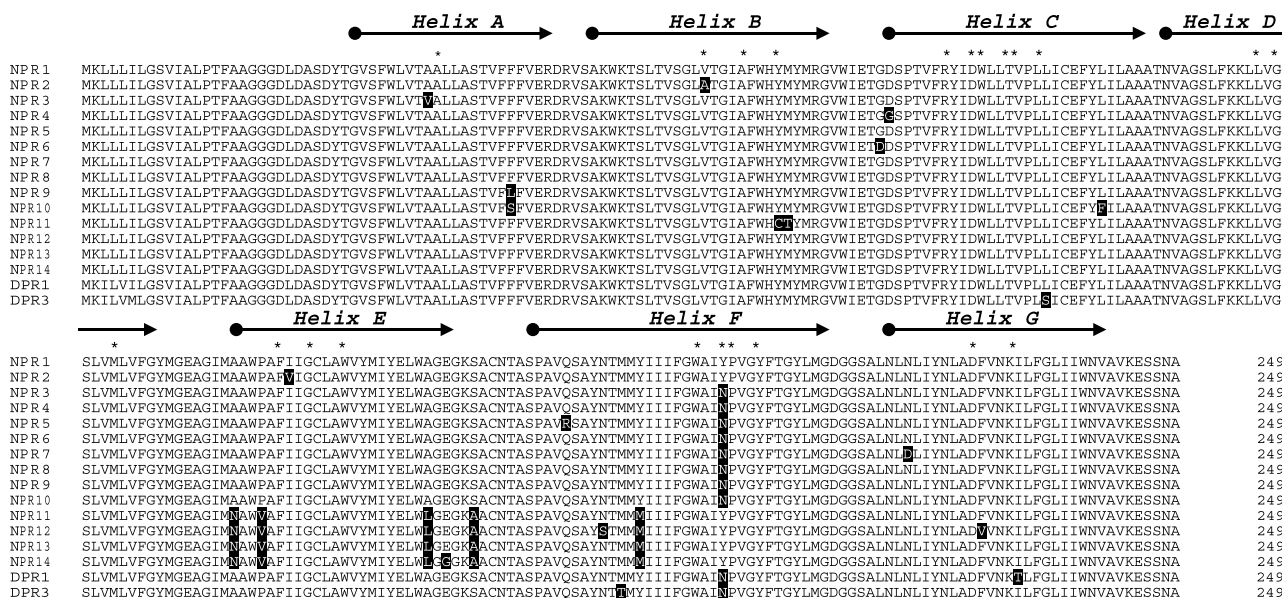


Fig. 1. Amino acid sequence comparison of 16 PRs from the Arctic Ocean. Differences between the PR variants are marked in black and the 22 residues of the retinal binding pocket are marked with asterisks. Predicted helices A–G are represented with black arrows and labeled with characters. NPR1 is identical to GPR from Monterey Bay (MBP), but was isolated from the Arctic Ocean.

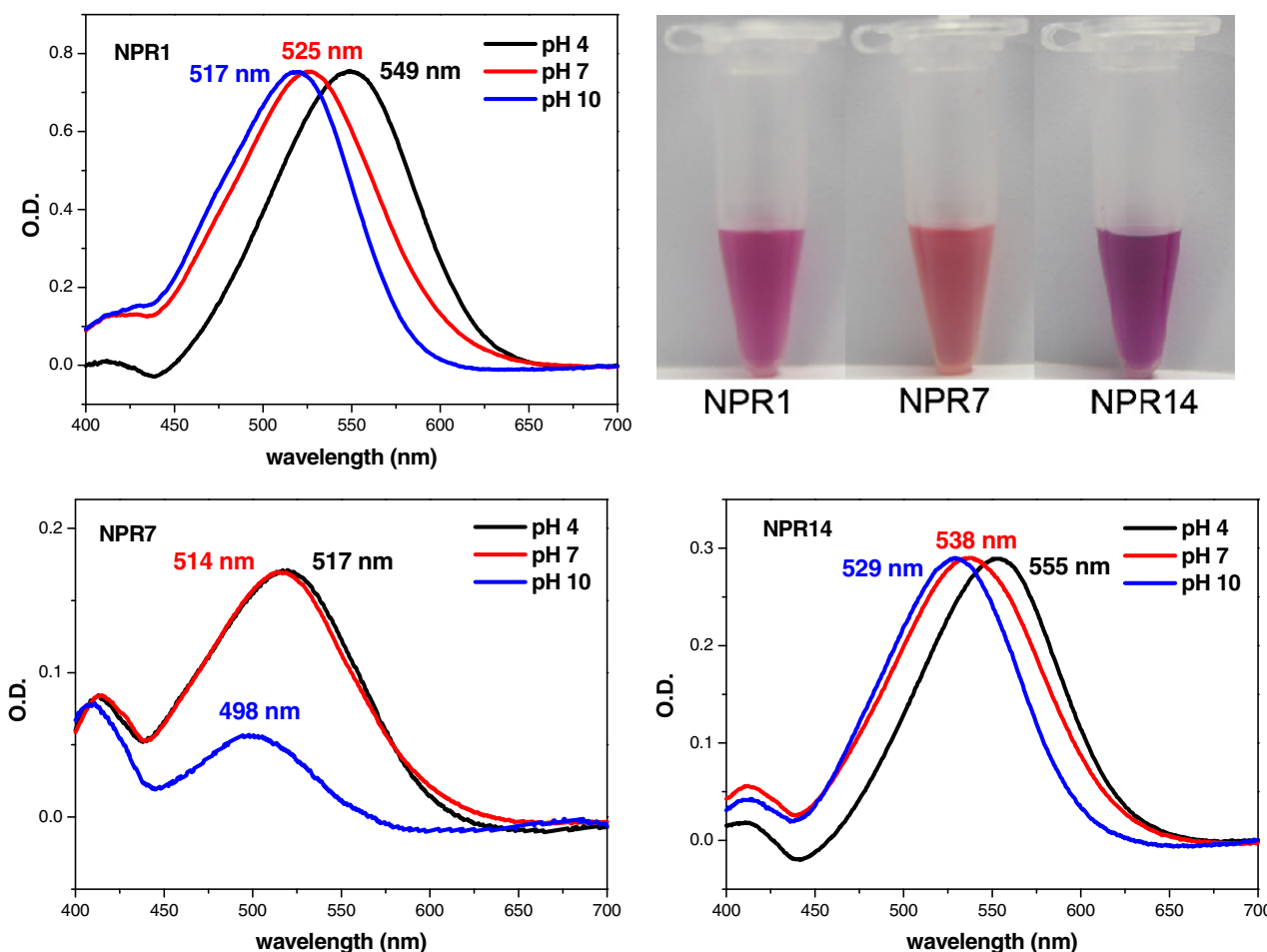


Fig. 2. Absorption spectra of NPR1, NPR7, and NPR14 at different pH values. Purified PR variants were in 50 mM Tris–HCl (pH 7.0), 150 mM NaCl, and 0.02% DM. NPR7 has the most blue-shifted absorption maximum and NPR14 has the most red-shifted absorption maximum.

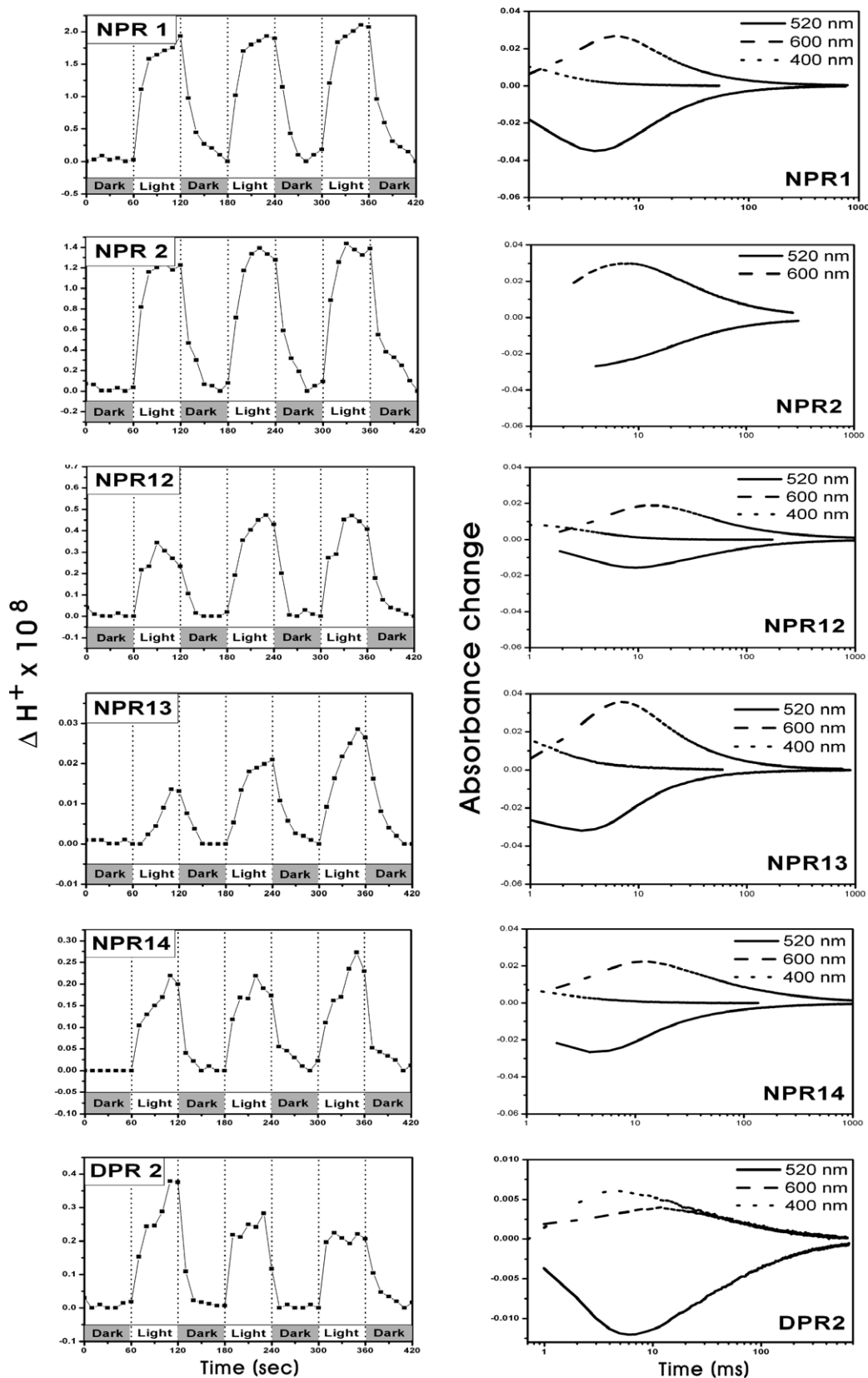


Fig. 3. The relationship between the pumping activity and rate of the photochemical reactions. The left six panels show proton transporting activities of PRs and the right six panels show photochemical reactions of PRs. On the left panel, >440 nm illumination was applied to spheroplasts for 60 s after 60 s in the dark period and this cycle was repeated three times. Initial pH values were adjusted to 7.8 to mimic the native environment. On the right six panels, the O formation and decay, return to the ground state, and the M decay were measured at 600, 520, and 400 nm, respectively.

the nine PRs blue-shifted at pH 10 have the 200th residue, the retinal binding site Tyr homologous to Tyr185 of bacteriorhodopsin, replaced by Asn. The PR variants were titrated to determine the pK_a of the major spectral transition corresponding to the deprotonation of the Schiff base counterion, and only a major pK_a is shown in Table 1. The titration of NPR1 fits well to a single pK_a of 7.5 (Table 1); however, a second minor component was also present in the NPR4, NPR6, DPR2, DPR3, and DPR4 variants (data not shown).

3.3. Many Arctic PRs have the photocycle rate slower than that in BPR

Although GPR exhibits fast O decay (<50 ms), 14 green absorbing PRs from the Arctic Ocean have slower O decay than that in BPR. Three PRs have fast O decay which is similar to GPR (Table 1). PRs with the relatively fast photocycling rate (NPR1, 2, 12, 13, 14, and DPR2) have ability to translocate protons in *E. coli* spheroplast upon illumination (Fig. 3). The proton efflux values for the rest of PRs (having relatively slow O decay) were not detected.

3.4. DPR2 and DPR4 are similar to other Arctic PRs

The absorption maxima of DPR2 and DPR4 at pH 10 are more similar to that of GPR, although their slow photocycle is more characteristic of BPR. According to the previously reports, GPRs on the surface waters have fast photocycles and BPRs in deeper waters have slow photocycles [3,9]. However, 14 PRs from the cold Arctic surface water have been identified in this study with slow rate of photocycling, suggesting that the photochemical properties of PR depend not only on the depth but also on the environmental temperature.

3.5. Comparing temperature dependencies of the photocycle rates of the Y200N variant, GPR, and BPR

We compared temperature dependency of the O decay rate of NPR8 (bearing Y200N replacement) with NPR1 (GPR) and BPR. There are subtle differences among the GPR, BPR, and Y200N variants. GPR shows somewhat lower

dependency of the photocycle turnover rate on the temperature than BPR, as judged from the slopes of the Arrhenius plots (Fig. 4). NPR8 presents the dependency intermediate between those of GPR and BPR. The slope ($\Delta H/R$) for NPR8 (−5082) is in the middle between those for GPR (−4430) and BPR (−5433). Also, the O decay in the Y200N variant has smaller ΔS of activation than in BPR and larger ΔS than in GPR. The NPR3 (A38V and Y200N replacements) and NPR9 (F47L and Y200N replacements) variants showed temperature dependencies of the O decay similar to that of NPR8 (data not shown).

4. Discussion

Until recently, proteorhodopsins from the Arctic Ocean were not studied, although PRs in the Antarctic, the Pacific ocean, and the Mediterranean sea are well-known in terms of their sequences, absorption maxima, and photochemical reactions [3,5,6,19,20]. We found that in contrast to a previous report that Pale6 in the Antarctic Ocean absorbs blue light ($\lambda_{max} = 490$ nm, pH 7), all PR variants in the Arctic Ocean absorb in the green light region and their amino acid sequences are similar to that of MBP [3]. While there is a relatively small number of PRs with the fast (MBP-like) photocycle in the Arctic Ocean, 14 out of the 18 Arctic PR variants isolated in this study showed photochemical reactions similar to or slower than that of BPR. Consequently, we suggest that PRs do not have a strict positive correlation between the absorption maximum and photocycling rate, as 77% of our PR isolates have very slow photocycle. It is possible that the reason for the existence of GPRs with slow photochemical kinetics in the surface of the cold ocean is to perform a function other than proton pumping, such as a signaling or regulatory function [9,21]. Recently, putative sensory PRs were identified based on a bioinformatic analysis, but their function remains thus far unknown [22,23]. Another possible reason for the presence of the inefficiently (slow) proton pumping PRs is that bacterioplankton in the cold ocean environment does not require as much energy production as compared with prokaryotes in warmer marine environments because the metabolic rate in cold sea water should be very slow.

The Y185F mutant of bacteriorhodopsin (BR), which is a homolog of Y200 of PR is replaced, is well-studied. The amino acid substitution Tyr-185 → Phe increased the lifetime of the photocycle (14-fold) [24,25], but this mutant successfully pumps proton [26]. Similar to the Y185F replacement in BR, the Y200N mutation (e.g., NPR8) increases the lifetime of the photocycle. The room temperature average relaxation time of the O intermediate for NPR8 (Y200N) is 29 times greater than the corresponding relaxation time for MBP and the decay time for the M intermediate is four times greater. The Y200N replacement elevates the activation entropy and enthalpy of the transition between the O intermediate and the ground state that becomes more dependent on temperature than in wild-type PR. It seems that the PR variants might modulate their photocycle rate to control the rate of proton pumping in response to environmental temperature changes so as to supplement a shortage of energy in an emergency case. For example, in low temperature marine environment bacteria may not need much energy, so they have low rate of the PR photocycle turnover. Since we have not detected proton pumping activity in

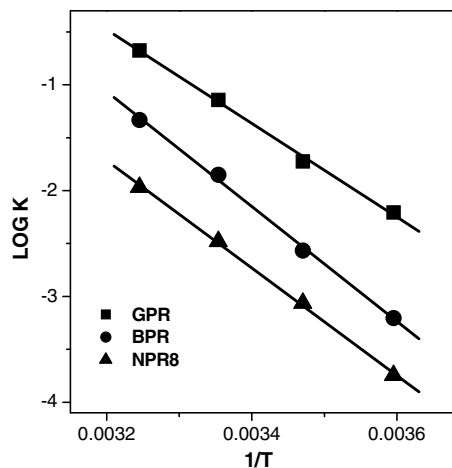


Fig. 4. Temperature dependence of the rate of the O decay in GPR, BPR, and NPR8. The half lives for the O decay were measured at 5, 15, and 35 °C, and the logarithms of the rates (the reciprocal of the half lives of O decay) were plotted against the reciprocal of the temperature. The data were fitted to a linear least squares lines, and the correlation coefficients were calculated; R^2 for each plot >0.99.

the Y200N variants at pH 7.8 due to either insufficient sensitivity of the method, or high pK_a of the Schiff base counterion, or slow photocycle rate, we cannot exclude the possibility that these proteins act as sensory rhodopsins.

Acknowledgements: The authors thank Prof. Leonid Brown for fruitful discussion. This work was supported by the Korea Research Foundation Grant (KRF 2004-042-C00113) and Seoul Research and Business Development Program (10816) to K.H. Jung, and a Grant PE08050 from Korea Polar Research Institute. J.Y. Jung and A.R. Choi were supported by the 2nd stage of Brain Korea 21 graduate Fellowship Program.

References

- [1] Brown, L.S. and Jung, K.H. (2006) Bacteriorhodopsin-like proteins of eubacteria and fungi: extent of conservation of the haloarchaeal proton-pumping mechanism. *Photochem. Photobiol. Sci.* 5, 538–546.
- [2] Bèjà, O., Aravind, L., Koonin, E.V., Suzuki, M.T., Hadd, A., Nguyen, L.P., Jovanovich, S.B., Gates, C.M., Feldman, R.A., Spudich, J.L., Spudich, E.N. and DeLong, E.F. (2000) Bacterial rhodopsin: evidence for a new type of phototrophy in the sea. *Science* 289, 1902–1906.
- [3] Bèjà, O., Spudich, E.N., Spudich, J.L., Leclerc, M. and DeLong, E.F. (2001) Proteorhodopsin phototrophy in the ocean. *Nature* 411, 786–789.
- [4] De la Torre, J.R., Christianson, L., Bèjà, O., Suzuki, M.T., Karl, D., et al. (2003) Proteorhodopsin genes are widely distributed among divergent bacterial taxa. *Proc. Natl. Acad. Sci. USA* 100, 12830–12835.
- [5] Man, D., Wang, W., Sabehe, G., Aravind, L., Post, A.F., Massana, R., Spudich, E.N., Spudich, J.L. and Bèjà, O. (2003) Diversification and spectral tuning in marine proteorhodopsins. *EMBO J.* 22, 1725–1731.
- [6] Sabehe, G., Loy, A., Jung, K.H., Partha, R., Spudich, J.L., Isaacson, T., Hirschberg, J., Wagner, M. and Bèjà, O. (2005) New insights into metabolic properties of marine bacteria encoding proteorhodopsins. *PLoS Biol.* 3, e273.
- [7] Sabehe, G., Massana, R., Bielawski, J.P., Rosenberg, M., DeLong, E.F., et al. (2003) Novel proteorhodopsin variants from the Mediterranean and Red Seas. *Environ. Microbiol.* 5, 842–849.
- [8] Sabehe, G., Bèjà, O., Suzuki, M.T., Preston, C.M. and DeLong, E.F. (2004) Different SAR86 subgroups harbour divergent proteorhodopsins. *Environ. Microbiol.* 6, 903–910.
- [9] Wang, W., Sineshchekov, O.A., Spudich, E.N. and Spudich, J.L. (2003) Spectroscopic and photochemical characterization of a deep ocean proteorhodopsin. *J. Biol. Chem.* 278, 33985–33991.
- [10] Morris, R.M., Rappe, M.S., Connon, S.A., Vergin, K.L., Siebold, W.A., et al. (2002) SAR11 clade dominates ocean surface bacterioplankton communities. *Nature* 420, 806–810.
- [11] Ulrich, S., Russell, A.D., Jang-Cheon, C., Kevin, L.V. and Stephen, J.G. (2007) The SAR 92 clade: an abundant coastal clade of culturable marine bacteria possessing proteorhodopsin. *Appl. Environ. Microbiol.* 73, 2290–2296.
- [12] Gómez-Consarnau, L., González, J.M., Coll-Lladó, M., Gourdon, P., Pascher, T., Neutze, R., Pedros-Alio, C. and Pinhassi, J. (2007) Light stimulates growth of proteorhodopsin containing marine Flavobacteria. *Nature* 445, 210–213.
- [13] Lee, Y.K., Sung, K.C., Yim, J.H., Park, K.J., Chung, H. and Lee, H.K. (2005) Isolation of protease-producing Arctic marine bacteria. *Ocean Polar Res.* 27, 215–219.
- [14] Lee, Y.K., Kim, H.W., Liu, C.L. and Lee, H.K. (2003) A simple method for DNA extraction from marine bacteria that produce extracellular materials. *J. Microbiol. Methods* 52, 245–250.
- [15] von Lintig, J. and Vogt, K. (2000) Filling the gap in vitamin A research. *J. Biol. Chem.* 275, 11911–11920.
- [16] Choi, A.R., Kim, S.Y., Yoon, S.R., Bae, K. and Jung, K.H. (2007) Substitution of Pro206 and Ser86 residues in retinal binding pocket of *Anabaena* sensory rhodopsin is not sufficient for proton pumping. *J. Microbiol. Biotechnol.* 17, 138–145.
- [17] Shi, L., Yoon, S.R., Bezerra, A.G., Jung, K.H. and Brown, L.S. (2006) Cytoplasmic shuttling of protons in *Anabaena* sensory rhodopsin: implications for signaling mechanism. *J. Mol. Biol.* 358, 686–700.
- [18] Boer, M., Graeve, M. and Kattner, G. (2006) Impact of feeding and starvation on the lipid metabolism of the Arctic pteropod *Clione limacine*. *J. Exp. Mar. Biol. Ecol.* 328, 98–112.
- [19] Kelemen, B.R., Du, M. and Jensen, R.B. (2003) Proteorhodopsin in living color: diversity of spectral properties within living bacterial cells. *Biochim. Biophys. Acta* 1618, 25–32.
- [20] Aharonovich, D.M., Sabehe, G., Sineshchekov, O.A., Spudich, E.N., Spudich, J.L. and Bèjà, O. (2004) Characterization of RS29, a blue-green proteorhodopsin variant from the Red Sea. *Photochem. Photobiol. Sci.* 3, 459–462.
- [21] Jung, K.H. (2007) The distinct signaling mechanisms of microbial sensory rhodopsins in Archaea, Eubacteria, and Eukarya. *Photochem. Photobiol.* 83, 63–69.
- [22] Spudich, J.L. (2006) The multitasking microbial sensory rhodopsins. *TIBS* 14, 480–487.
- [23] Venter, J.C. et al. (2004) Environmental genome shotgun sequencing of the Sargasso Sea. *Science* 304, 66–74.
- [24] Ahl, P.A., Stern, L.J., Mogi, T., Khorana, H.G. and Rothschild, K.J. (1989) Substitution of amino acids in helix F of bacteriorhodopsin: effects on the photochemical cycle. *Biochemistry* 28, 10028–10034.
- [25] Sonar, S., Krebs, M.P., Khorana, H.G. and Rothschild, K.G. (1993) Static and time-resolved absorption spectroscopy of the bacteriorhodopsin mutant Tyr-185 → Phe: Evidence for an equilibrium between bR₅₇₀ and an O-like species. *Biochemistry* 32, 2263–2271.
- [26] Mogi, T., Stern, L.J., Hackett, N.R. and Khorana, H.G. (1987) Bacteriorhodopsin mutants containing single tyrosine to phenylalanine substitutions are all active in proton translocation. *Proc. Natl. Acad. Sci. USA* 84, 5595–5599.